Composites Science and Technology 257 (2024) 110806

Contents lists available at ScienceDirect

Composites Science and Technology

journal homepage: www.elsevier.com/locate/compscitech

Degradation kinetics of PLA/hemp biocomposites: Tradeoff between nucleating action and pro-hydrolytic effect of natural fibers

Libera Vitiello [a], Sabrina Carola Carroccio [b], Veronica Ambrogi [a], Edoardo Podda [c], Giovanni Filippone [a,*], Martina Salzano de Luna [a]

[a] Dipartimento di Ingegneria Chimica, Dei Materiali e Della Produzione Industriale (UdR Naples, INSTM Consortium), Università di Napoli Federico II, Piazzale Tecchio 80, 80125, Naples, Italy
[b] Institute for Polymers, Composites and Biomaterials IPCB-CNR, Via P. Gaifami 18, 95126, Catania, Italy
[c] Dipartimento di Scienze e Innovazione Tecnologica, Università Del Piemonte Orientale, Viale T. Michel 11, 15121, Alessandria, Italy

ARTICLE INFO

Keywords:
Natural fibers (A)
Particle-reinforced composites (A)
Bio composites (A)
Environmental degradation (B)
Differential scanning calorimetry (DSC) (D)

ABSTRACT

Natural fibers are not only a sustainable alternative to synthetic reinforcement materials, but can also be used to produce truly sustainable biocomposites with fast degradation kinetics. Indeed, due to their hygroscopicity, lignocellulosic fibers allow water and/or degrading organisms from the external environment to penetrate inside the host matrix and trigger its hydrolysis. The latter is the rate-limiting step for the degradation of bio-polyesters, which exhibit unacceptably slow degradation kinetics at ambient temperature and humidity. However, fibers also promote crystallization of the host matrix and thus slow down its degradation kinetics. To better understand and potentially control the degradation kinetics of biocomposites, here we investigate the ability of hemp shives, a hygroscopic by-product of hemp fiber production, to accelerate the hydrolysis of poly (lactic acid) (PLA). The degradation kinetics and degree of crystallinity of PLA are monitored in water and mature compost as a function of fiber content, which was varied across the percolation threshold (Φ_c) to study the effect of fiber interconnectivity. Above Φ_c, the fibers accelerate PLA hydrolysis in water despite their nucleating effect. Conversely, in compost the shielding effect of fiber-induced crystallinity prevails, and the fibers eventually slow down the degradation kinetics of PLA.

1. Introduction

Compared to conventional petroleum-based plastics, biopolymers have the inherent advantage of being made from renewable resources and, more importantly, being biodegradable or compostable [1–4]. However, contrary to what is often claimed, the biodegradation of such materials in the natural environment can be a very slow process, which has obvious implications for their actual environmental impact. The challenge is to shorten the biodegradation time while maintaining the environmental friendliness of the materials and the excellent properties of plastics. One of the most promising biodegradable polymers currently on the market is polylactic acid (PLA), a bio-based aliphatic polyester derived from starch raw materials such as corn starch, tapioca roots, chips or starch and sugarcane. Although its hydrolysable backbone, PLA biodegradation is a complex process that can be unacceptably slow [5]. It consists of an abiotic process, in which the ester bonds along the backbone of the PLA chain are hydrolytically cleaved to form lower molecular weight molecules, followed by a biotic degradation process, in which microorganisms assimilate and mineralize the degradation products, releasing elements such as carbon dioxide, water, and biomass into the environment [5,6]. The polymer chains can only penetrate the cell membrane of microorganisms if their molecular weight reaches 10–20 kDa [5–7]. In other words, abiotic hydrolysis can be considered as the rate-limiting step of PLA biodegradation [8]. One possible strategy to accelerate this critical step is compounding PLA with specific fillers able to promote hydrolysis [9–11]. In this context, lignocellulosic fillers are receiving increasing attention due to their eco-friendliness, wide availability, and effectiveness in transporting water molecules into the host matrix through their hemicellulose fraction. In addition, their swelling in a humid environment could lead to filler-matrix debonding, facilitating the access of water through capillary effects and further accelerating the hydrolysis of the host PLA [12–15]. To enhance these mechanisms, the degree of interconnectivity of the particles is important. The access of water molecules from the external environment is

* Corresponding author.
E-mail address: gfilippo@unina.it (G. Filippone).

https://doi.org/10.1016/j.compscitech.2024.110806
Received 15 May 2024; Received in revised form 5 July 2024; Accepted 9 August 2024
Available online 10 August 2024

indeed easier when the particles form a continuous path that connect the surface and the interior of the composite. However, apart from some notable exceptions [16–19], the role of the filler content and, more specifically, of the fiber volume fraction at which the percolation threshold is reached (Φ_c), is neglected. Moreover, even when the relevance of Φ_c is recognized, possible nucleating effects of the filler are not properly addressed. The crystalline domains are much more resistant to hydrolysis than the amorphous regions. Moreover, crystallization reduces water diffusivity, possibly slowing down the hydrolysis kinetics. To complicate matters, crystallinity varies during the PLA degradation [20,21], making the overall effect of natural fillers on the abiotic degradation of the PLA difficult to predict. To shed light on this complex matter, here we study the degradation kinetics of PLA-based biocomposites filled with natural short fibers (average length <500 μm, average length-to-diameter ratio <5) obtained from hemp shives, a by-product of the hemp fiber production obtained from the woody inner portion of the hemp stalk. The reason for this choice is that this less noble fraction of the hemp plant is rich in hemicellulose, which is mainly responsible for the moisture absorption of lignocellulosic fillers [12]. The goal was indeed to promote the transport of water molecules from the external environment and trigger the abiotic hydrolysis essential for PLA biodegradation. Such a pro-degradative action of the hemp shives was systematically studied by monitoring the evolutions of degree of crystallinity and molecular weight of PLA in two different environments, i.e. water and mature green compost. The role of filler content was investigated, focusing on the effect of the percolation threshold. Non-monotonic trends with filler content and opposite effects in water and soil were revealed. Overall, our results contribute in the understanding the complex interplay among the different parameters investigated, providing useful guidelines for the rational design of truly sustainable PLA-based products that also consider end-of-life issues.

2. Materials and methods

2.1. Materials

PLA is a commercially available poly (L-lactide-co-D-lactide) random copolymer with 4 % D-isomer, marketed by Corbion under the trade name Luminy® LX175. It has a density of $\rho_m = 1.24$ g/cm^3 and a melt flow index of MFI = 6 g/10 min (T = 210 °C and 2.16 kg). The average molecular weight of the unprocessed PLA pellets is $M_w = 126.6$ kDa ($M_w/M_n = 1.5$). Hemp shives were provided by Equilibrium S. r.l. (Nibionno, Italy) and contain about 44.3 % cellulose, 27.2 % hemicellulose, 22 % lignin and 6.2 % other elements [22]. The hemp was ground to a fine powder, hereinafter referred to as "fibers", by using a Retsch cutting mill (Retsch, Haan, Germany) with a pitch of 0.25 mm. The so obtained fibers were in the form of short-capped cylinders with volume average length of 376 ± 181 μm [23]. Their true density, measured with a helium pycnometer (AccuPyc II 1340, Micromeritics-Alfatest, Italy), was $\rho_f = 1.51$ g/cm^3.

2.2. Sample preparation

A Brabender Pantograph EC batch mixer (Brabender GmbH & Co. KG, Germany) was used to prepare samples with a nominal filler content (Φ) of 5–30 vol%. Before mixing, the PLA was dried overnight at 85 °C under vacuum and the natural fibers were conditioned at 25 °C and 80 % RH reaching a moisture content of 9.5 wt% (see Supplementary material, section S1). Melt compounding was carried out at 180 °C and 60 rpm for 6 min. The material was then molded into square plates (10 × 10 × 0.3 cm^3) using a hydraulic press (20 MT, Lab Tech Engineering Company LTD). The material, sandwiched between two Teflon sheets, was placed in the mold, preheated to T = 180 °C and softened for 5 min without pressure. Then the pressure was increased to ~15 MPa and kept constant for 4 min. Finally, the mold was cooled to ~40 °C under constant pressure. The resulting plates were cut into rectangular specimens (3 × 1 × 0.3 cm^3) using a circular saw.

2.3. Degradation in fresh water

The specimens were immersed in test tubes containing 50 mL of water (pH ≈ 7.5) and kept at T = 45 °C with gentle stirring in a shaking incubator (Bormarc Shaker SKI 4). Before subsequent characterization, the samples were collected at fixed time intervals and carefully dried until reaching a constant weight.

2.4. Degradation in mature compost

The specimens were buried in mature green compost (water holding capacity 80 %, moisture content 55 %, pH = 6.6 (see Supplementary material, section S2);) and kept in an incubator (Bormarc Shaker SKI 4) at T = 55 °C and 20 % RH. The samples were collected at fixed times and subjected to the following analyses.

2.5. Characterization

Optical microscopy was performed using an Olympus BX53 M microscope (Olympus Corporation, Shinjuku, Japan). To observe the fibers, they were suspended in a polyvinyl alcohol solution and a drop of the resulting suspension was poured onto a glass slide. The surface morphology of the composites was also inspected in reflection mode. Scanning electron microscopy (SEM, model Leica 420 from Leica, Wetzlar, Germany) was used to examine the internal microstructure of the samples. Prior to the observations, the specimens were brittle fractured after cooling to about −80 °C and the surfaces were coated with a thin layer of gold. Size exclusion chromatography (SEC) was performed using a 590 Waters chromatograph equipped with Waters HSPgel HR3 and HR4 columns and a refractive index detector. Measurements were performed in tetrahydrofuran (THF) at a flow rate of 0.3 mL/min. The weight-average molecular weight (M_w) and polydispersity index (M_w/M_n) were derived from the calibration curve based on PS standards (ranging from 370 g/mol to 100,000 g/mol). Differential scanning calorimetry (DSC) was performed using a TA Instrument DSC Q2000. The analyses were carried out under nitrogen flux (50 mL/min) on 12 ± 2 mg samples in non-hermetically sealed aluminum pans. The samples were heated from room temperature to 200 °C at 10 °C/min. The glass transition temperature (T_g) and the onset temperature and enthalpy of cold crystallization (T_{cc}, ΔH_{cc}) and melting (T_m, ΔH_m) were recorded. The data were used to calculate the degree of crystallinity originally present in the samples (χ_C) using the following equation:

$$\chi_C = \frac{\Delta H_m - \Delta H_{cc}}{\Delta H_m^0 \times \left(1 - m_p/100\right)} \quad (1)$$

where ΔH_m^0 is the latent heat of crystallization of fully crystalline PLA (equal to 93.0 J/g [24,25]) and m_p is the weight percentage of the fibers.

3. Results

3.1. Fiber distribution and matrix crystallinity

To clarify the degradation mechanisms of the composites, it is first necessary to obtain a clear picture of their microstructure in terms of fiber distribution and polymer crystallinity. The distribution of fibers is shown in Fig. 1. The hemp fibers appear as thick bundles of thin fibrils randomly oriented in the PLA matrix (Fig. 1a and b). The presence of isolated fibrils suspended in the matrix is occasionally noticed. The fiber percolation threshold, estimated in a previous work by means of dielectric spectroscopy and rheological analyses [23], is $\Phi_c = 10.1$ %. This means that a continuous three-dimensional network of hemp fibers is embedded in the PLA matrix in the samples with $\Phi \geq 15$ %. Conversely, the samples with 5 % and (at the limit) 10 % can be depicted

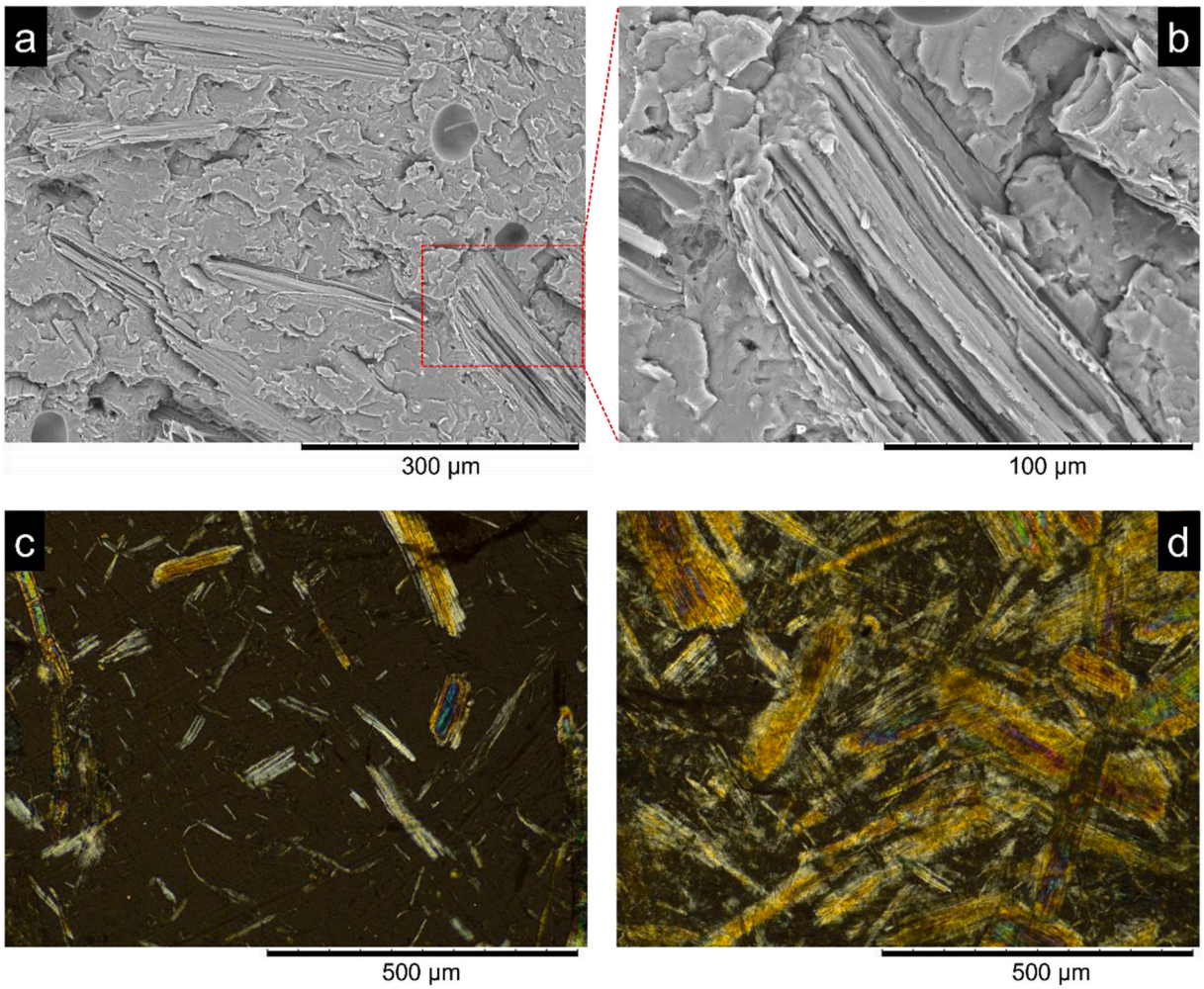

Fig. 1. a, b) SEM micrographs of the sample at 20 % of fibers (b is a magnification of the fibers in the red box in a). c, d) Polarized optical micrographs of the as-prepared samples at $\Phi = 5$ % (c) and $\Phi = 20$ % (d). The polymer matrix appears dark.

as a suspension of fibers and fiber aggregates in the host polymer. Polarized optical micrographs of two samples below and above Φ_c are shown in Fig. 1c and d.

The SEC analyses, summarized in Table 1, indicate an overall slight decrease in molecular weight compared to unprocessed PLA. The lack of a trend with fiber content suggests that the observed degradation is essentially due to the thermomechanical stresses during processing and not an effect related to the presence of the fibers.

The effect of hemp fibers on PLA crystallinity was investigated using DSC. The DSC curves (first heating scans) of the as-prepared samples are shown in Fig. 2 With an apparent slight decrease with fiber content (Fig. 3(a)). The onset of cold crystallization is between 95 and 100 °C and is slightly lower for the composites with higher fiber content (Fig. 3 (b)). The melting process is also slightly anticipated by the presence of the fibers, indicating the presence of a fraction of small and/or imperfect crystals in the composites that melt at lower temperatures (Fig. 3(c)).

Table 1
Average molecular weight and polydispersity indices of unprocessed PLA and several composites at different fiber content.

Sample	M_w [kDa]	M_w/M_n
Unprocessed PLA (pellet)	126.6	1.5
Processed PLA	113.9	1.6
PLA+10 % hemp	110.3	1.4
PLA+20 % hemp	100.8	1.6
PLA+30 % hemp	113.6	1.5

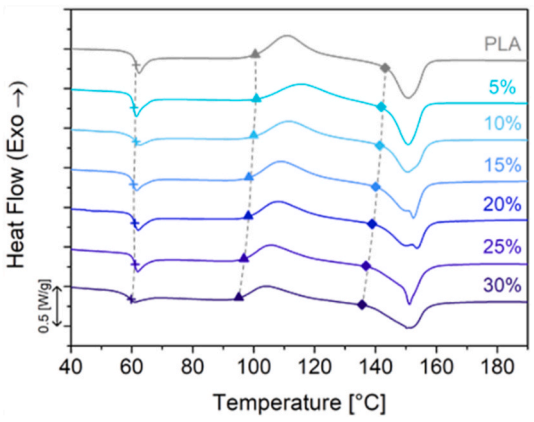

Fig. 2. DSC thermograms (first heating scan) of the as prepared PLA and composites with different fiber content.

Fig. 2 shows that the composites with intermediate fiber content ($10 \leq \Phi \leq 20$ %) exhibit a peculiar splitting of the melting peak into two distinct signals, which are attributed to the coexistence of different crystalline forms [26–28] and/or to the occurrence of melting-recrystallization phenomena during heating [27]. As for the crystallinity initially present in the samples (Fig. 3(d)), which is of particular interest to us as it could influence the degradation kinetics of

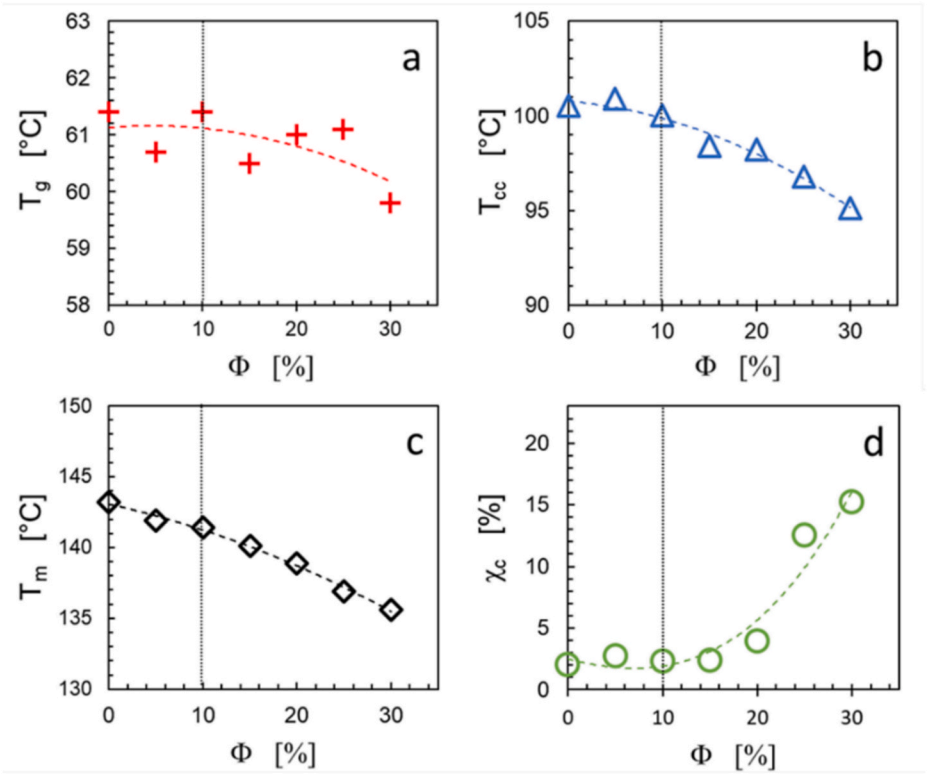

Fig. 3. Glass transition temperature (a), onset temperature of cold crystallization (b), melting (c), and degree of crystallinity (d) of the as prepared samples as a function of fiber content. The dashed lines are guides for the eye; the vertical dotted lines indicate the threshold of fiber percolation (10.1 %).

the samples, it is negligible (<3 %) in the samples at $\Phi \leq 15$ %, then a significant increase in χ_c is observed. This fiber-induced crystallization starts above Φ_c, i.e. when the fibers are densely packed and the effects of polymer confinement become relevant. Fiber distribution and matrix crystallinity affect both mechanical properties and degradation kinetics. The former aspect goes beyond our current purpose, yet preliminary flexural tests indicate that the fibers, although not intended for reinforcement purposes, promote a slight increase of the flexural modulus coupled with a decrease in the strength and elongation at break (see Supplementary material, Section S3). Regarding the degradation kinetics, since the hydrolytic degradation of PLA is hindered by crystallinity [28], the effect of fibers is more complex than one would expect.

3.2. Degradation in freshwater

The macroscopic appearance of the samples after 50 days of soaking in freshwater is shown in Fig. 4(a). The neat PLA sample, initially transparent, rapidly becomes opaque after immersion. Opacity is a degradation consequence and can be linked to various phenomena. These include light scattering due to the presence of microvoids, water and/or degradation products formed during the hydrolytic process. An increase in crystallinity is also possible due to the higher chain mobility caused by the degradation itself and/or by a plasticizing effect of the water [29,30]. The same mechanisms also occur in the PLA matrix of the composites. Overall, no macroscopic damage was observed after 50 days of soaking. However, optical photomicrographs show some surface erosion in all samples, evidenced by the disappearance of the geometric pattern imprinted by the Teflon films used during hot compression

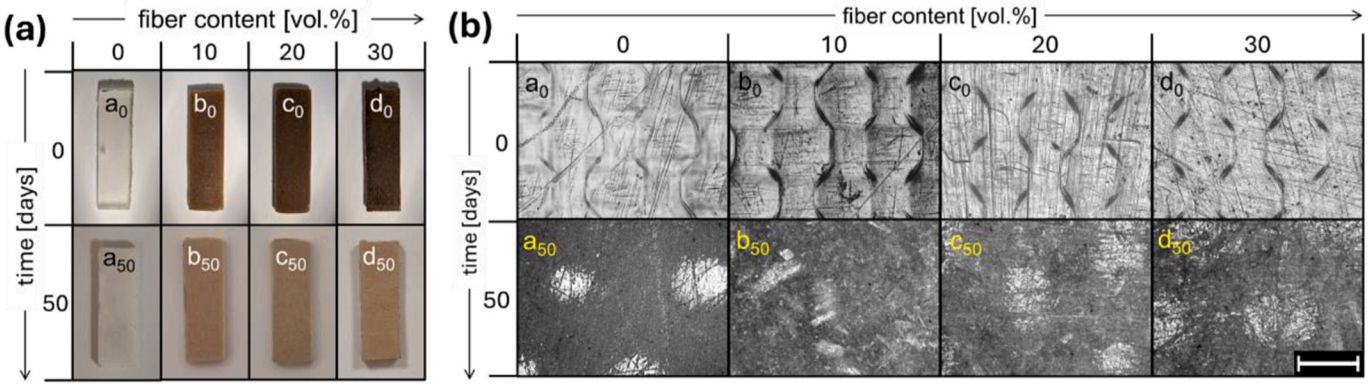

Fig. 4. (a) Pictures of the samples with different fiber content after 50 days of soaking in freshwater. (b) Optical micrographs showing the surfaces of selected specimens. The geometric pattern in PLA and composites before the water soaking reflects the texture of the release fabric used during hot compaction. The scale bar, common to all micrographs, corresponds to 500 μm.

(Fig. 4(b)).

The low temperature and the absence of exogenous microorganisms in the water medium chosen for the experiments lead to abiotic hydrolytic degradation of the PLA matrix in the studied composites. In pure PLA, this process follows a two-stage mechanism [29]. First, random hydrolytic scission of the ester bonds occurs with the diffusion of water molecules into the amorphous regions. In this initial phase, an increase in the degree of crystallinity is observed for two reasons: (i) a part of the amorphous domains transforms into crystals due to the increased free volume resulting from chain scission; (ii) a possible dissolution in the aqueous environment of the oligomers formed in the amorphous fraction. After this first step has progressed far enough, hydrolysis begins to attack the crystalline domains, progressing from the edge towards the center [21,31].

The same sequence can be assumed for the studied systems. In our case, however, the water molecules are also transported through the fibers by capillarity and diffusion mechanisms, reaching the interior of the samples and triggering hydrolysis. This is confirmed by the SEC measurements. The average molecular weight after 50 days of immersion in freshwater is shown in Table 2 for pure PLA and composite samples with different fiber content. Considering that low molecular weight fractions could have dissolved in water [9,32], the data, collected on solid samples, may be overestimated. The higher the fiber content, the lower the molecular weight. A comparison with Table 1 shows that the sample with the highest fiber content exhibits the greatest decrease in M_w (>40 %). Despite fiber interconnection, no discontinuities are observed when the percolation threshold ($\Phi_c = 10.1$ %) is exceeded. Further interesting information about the degradation process emerges from the DSC analyses after immersion (Fig. 5). We only referred to the first heating scan, which is representative of the status of the samples after immersion. The characteristic temperatures of the individual transitions and the degree of crystallinity are shown in Fig. 6 as a function of the fiber content. The T_g increases slightly after immersion in freshwater (Fig. 6(a)), indicating a greater compactness of the amorphous phase. The effect is much more relevant on T_{cc}, which decreases by more than 10 °C for all samples (Fig. 6(b)). The decrease in molecular weight and a certain plasticizing effect of water confer mobility to the polymer chains so that they start to cold-crystallize at lower temperatures. The higher chain mobility also affects the crystalline phase. The common onset of melting (~141 °C) and the similar shape of the melting peak, with a shoulder at ~150 °C followed by a deeper peak at ~155 °C (see Fig. 5), indicate that the crystals after immersion in water are more uniform and stable than those present in the untreated samples. What has clearly changed is the overall degree of crystallinity (Fig. 6(d)). The samples can be divided into two groups: those with Φ<15 %, where χ_c increases after immersion in water, and the samples with Φ>15 %, where the χ_c values are lower than before immersion. Interestingly, the critical fiber load at which the trend changes is the same at which the fibers started to have a nucleating effect before immersion in water, i.e. above $\Phi_c = 10.1$ %.

After immersion, an increase in crystallinity is expected, since the observed decrease in molecular weight (see Tables 1 and 2) gives the chains the necessary mobility to fold and crystallize [24]. Since hydrolysis starts in the amorphous phase, and considering that some solubilization of the formed oligomers could take place in the water environment, the increase in χ_c reflects the decrease in the amorphous fraction. Such an effect is evident in the unfilled PLA, but it gradually decreases in the presence of the fibers and finally disappears at $\Phi \approx 15$ %. Above this threshold, χ_c decreases after immersion in water. This means that at a sufficiently high fiber content, hydrolysis becomes particularly effective and begins to attack even the crystalline domains. The decrease in the degree of crystallinity becomes evident well above $\Phi_c = 10.1$ %. This means that the phenomenon occurs when a tangled fiber network connects the surface and the innermost parts of the material, providing additional access routes for water molecules from the environment to trigger hydrolysis. The mechanism of water adsorption in biocomposites was studied by Azwa et al. [12]. First, the water penetrates the fibers and binds to their hydroxyl groups until saturation. This causes the fibers to swell, which leads to stresses and microcracks at the fiber-matrix interface. Water-soluble substances begin to be released from the fibers and osmotic pressure pockets form, causing further fiber-matrix debonding. The reduction in fiber-matrix interfacial adhesion favors the access of additional water and, if present, biological and/or chemical species responsible for accelerating hydrolysis. It is reasonable that such a process is favored well above Φ_c. In other words, for hydrolysis to effectively attack the crystalline phase as well, it is not sufficient for the fibers to just touch each other, but a well tangled fiber network must form.

Table 2
Average molecular weight and polydispersity indices of PLA composites with different hemp content immersed in freshwater for 50 days.

Φ [vol%]	0	5	10	15	20	25	30
M_w [kDa]	85,8	84,8	80,6	79,5	79,1	76,5	69,4
M_w/M_n	1.61	1.60	1.60	1.60	1.61	1.60	1.63

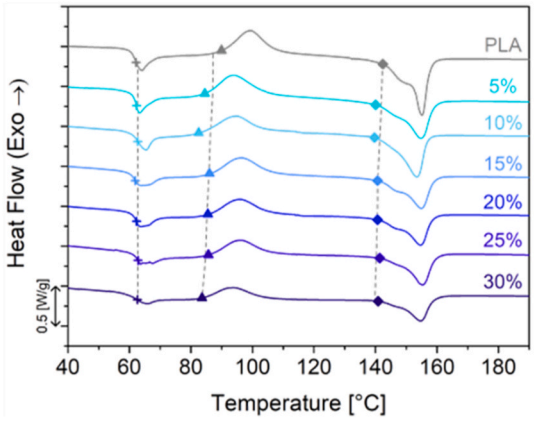

Fig. 5. DSC thermograms (first heating scan) of hemp shive-based composites at different fibre content after 50 days of water soaking.

3.3. Degradation in mature compost

In contrast to the samples immersed in water, the appearance changed significantly after burial in mature compost. Digital images of the samples during burial are shown in Fig. 7(a); optical micrographs of the surface of selected samples are shown in Fig. 7(b). During the first 10 days, the pure PLA undergoes a transition from transparent to opaque (Fig. 7(a), a_0 vs. a_{10}) due to light scattering phenomena caused by crystallinity, water and/or degradation products, holes and cracks that form in the bulk of the sample [29,33]. Surface erosion does not yet appear to have taken place, and the geometric pattern imprinted by the release fabric used during hot compaction is still clearly visible (Fig. 7 (b), a_0 vs. a_{10}). In the composites, only a color change can be observed on a macroscopic level after 10 days (Fig. 7). On closer inspection, however, the surface pattern is no longer visible (Fig. 7(b), b_{10}, c_{10} and d_{10}), which indicates premature surface erosion. It is difficult to detect differences between the composites with different fiber content. Surface erosion is particularly evident in the sample with $\Phi = 30$ % (Fig. 7(b), d_{10}), where exposed hemp fibers are clearly visible. The differences between the samples progressively vanish during burial. After 40 days, the first cracks appear on a macroscopic level in all samples (Fig. 7(a)), and surface erosion is also visible in the PLA sample (Fig. 7(b), a_{40}). Finally, after 100 days, all samples are thinner, surrounded by a sticky layer of organic material, and fragmented. Interestingly, the extent of fragmentation is higher for pure PLA (Fig. 7(b), a_{100}). It is possible that the fibers in the composites hold the pieces of matrix together,

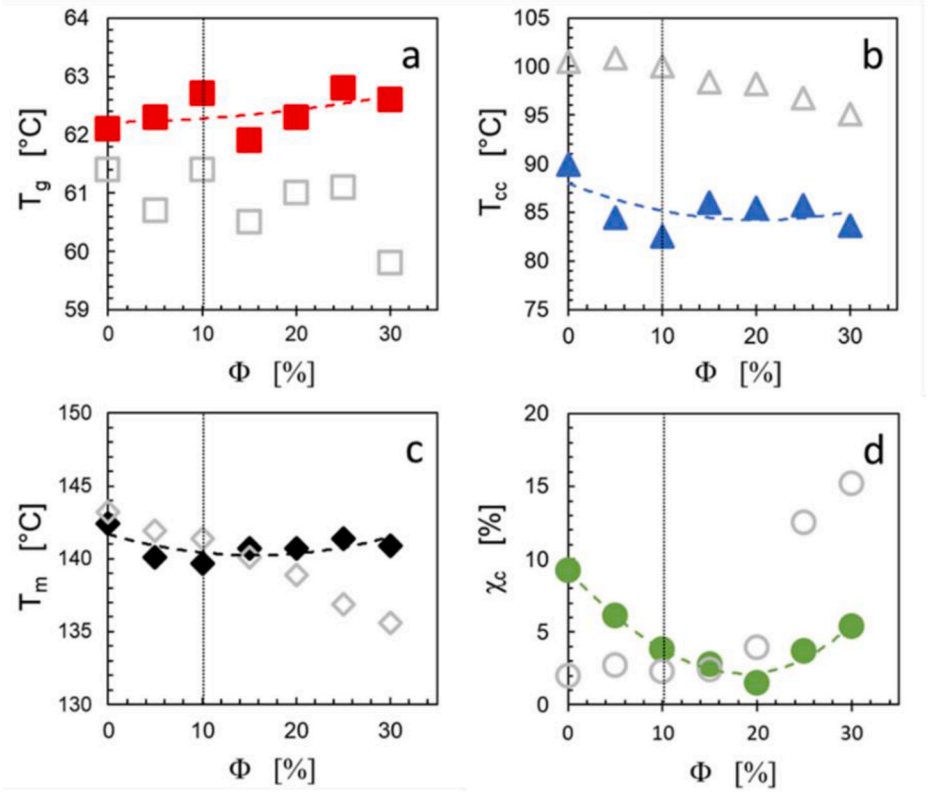

Fig. 6. Glass transition temperature (a), temperature of onset of cold crystallization (b), melting (c), and degree of crystallinity (d) of the samples as a function of fiber content for samples stored in water at T = 45 °C for 50 days. Empty symbols in light gray are the data before immersion in water (same as in Fig. 3). The dashed lines are guides for the eye; the vertical dotted lines indicate the fiber percolation threshold (10.1 %).

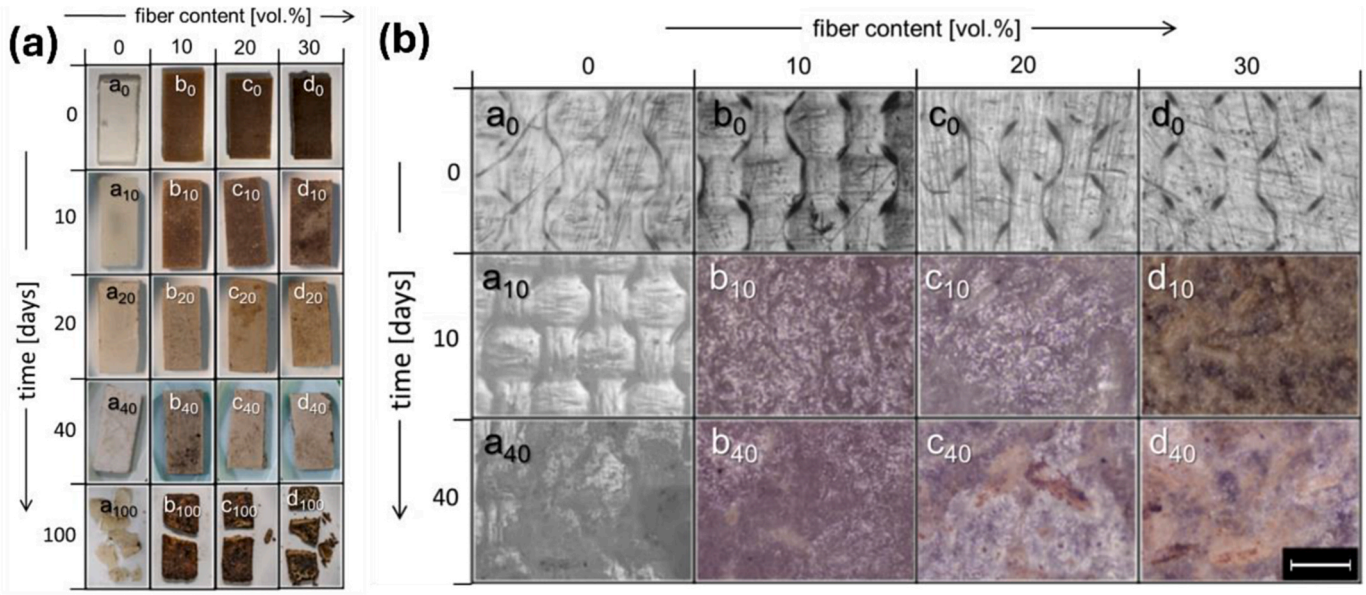

Fig. 7. (a) Images of the samples with different fiber content buried for different time intervals. (b) Optical micrographs of the surfaces of selected specimens. The geometric pattern in PLA and composites before burial reflects the texture of the release fabric used during hot compaction. The scale bar, common to all micrographs, corresponds to 500 μm.

preserving the integrity of the samples.

Visual inspection of the samples suggests that the fibers accelerate degradation, at least in the early stages of burial, when surface erosion has clearly occurred in the composites but not in the pure PLA (Fig. 7(b), a_{10} vs. b_{10}, c_{10}, d_{10}). Nothing can be said about longer burial times where all samples appear comparably degraded. To obtain more quantitative information, SEC analyses were performed. The evolution of the molecular weight distributions as a function of burial time is shown in Fig. 8. The average molecular weights are given in Table 3. Note that the data for the samples buried for 40 days suffer from the low representativeness of average values for multimodal distributions (see Fig. 8(c)). Comparison with Table 2 shows that the PLA degrades much faster in

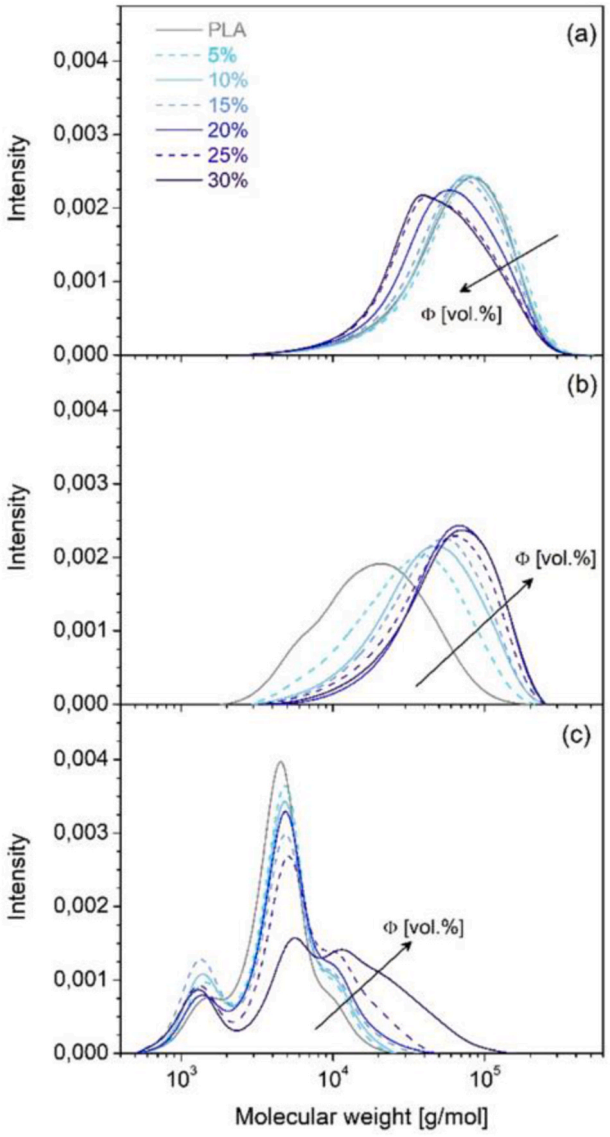

Fig. 8. SEC chromatograms of pure PLA and composites with different volumetric fiber content after 10 (a), 20 (b), and 40 (c) days in compost.

Table 3
Average molecular weight and polydispersity indices of PLA composites buried in mature compost for different time.

Φ [vol %]	burial time [days]							
	0 (before burial)[a]		10		20		40[b]	
	M_w [kDa]	M_w/M_n	M_w [kDa]	M_w/M_n	M_w [kDa]	M_w/M_n	M_w [kDa]	M_w/M_n
0	113.9	1.6	83,2	1.73	24,8	1.84	4,8	1.45
5			89,4	1.71	41,0	1.83	5,1	1.54
10	110.3	1.4	84,3	1.68	53,6	1.75	5,2	1.64
15			78,7	1.71	56,3	1.69	5,4	1.85
20	100.8	1.6	73,1	1.74	71,8	1.55	6,2	1.72
25			67,4	1.76	63,4	1.71	7,2	2.07
30	113.6	1.5	65,6	1.76	70,3	1.63	14,0	3.34

[a] Same data as in Table 1.
[b] Average values after 40-day burial suffer from the low representativeness of the average values for multimodal distributions.

compost than in freshwater. This is not unexpected and is related to the biotic environment and the higher temperature during composting. Looking at the effect of the fibers, they slightly accelerate degradation at 10 days, while the opposite is true for longer burial times. This agrees with the picture emerged from the visual inspection of the samples. The decrease in molecular weight is self-catalyzed and accelerates when M_w falls below a critical value M_c, at which the degraded chains begin to dissolve in the host environment [5]. Stloukal et al. estimated M_c~20 kDa for PLA in soil [9]. The data in Table 3 show that this threshold is reached in about 20 days for pure PLA, while longer burial times are needed as Φ increases. However, degradation remains fast also for the composites, which reach M_c in a time between 20 and 40 days. After 40 days, the presence of three main populations of short (~2 kDa), medium (5 kDa) and high (>10 kDa) molecular weight chains is detected. It should be noted that SEC analyses performed after long burial times are affected by the possible solubilization of part of the polymer in the environment. This low molecular weight fraction, hence, is not accounted in the analysis. Nevertheless, it is clear that the fibers slow down the degradation kinetics, and that the effect is particularly relevant at high fiber content. To interpret this behavior, which is in contrast with that observed in freshwater, the evolution of the molecular weight of the buried samples must be correlated with their degree of crystallinity.

The DSC curves of selected samples below and above Φ_c after 10, 20 and 40 days of burial are shown in Fig. 9(a–d). The evolution of T_m (Fig. 9(e)) and χ_c (Fig. 9(f)) is also shown. The most obvious effect of burial is the disappearance of the cold crystallization peak. This means that the endothermic signals recorded even after only 10 days of burial can be attributed exclusively to the melting of (i) the crystalline phase initially present in the buried samples, and (ii) of a secondary crystalline phase based on the oligomeric fractions formed during composting [34]. Since the first contribution is negligible for the pure PLA and the composites with Φ = 10 % (see Fig. 3(d)), the melting process of these samples is exclusively due to the secondary crystalline phase. Its amount increases significantly with time (Fig. 9(e)), reflecting the rapid progression of degradation emerged from the SEC analyses. In addition, the decrease in T_m with the burial time (Fig. 9(e)) indicates that the newly formed crystalline phase becomes increasingly unstable. In contrast, the crystallinity of the samples with Φ = 20 % and 30 % increases slowly and is much more stable. Since these samples originally had a non-negligible amount of crystallinity (Fig. 3(d)), it can be concluded that the slower degradation kinetics of the composites with high Φ is due to the shielding effect of fiber-induced crystallinity, which limits water diffusion and prevents the amorphous fractions from hydrolysis. In other words, in mature compost, the role of fibers as water carriers is only effective in the early stages of burial. Over longer times, the shielding effect of fiber-induced crystallinity prevails and the degradation kinetics slows down.

4. Conclusions

The effect of short hemp fibers on the degradation in freshwater and mature compost was investigated by combining DSC measurements and SEC analyses. The fiber content was varied from 5 to 30 vol%, i.e. above the fiber percolation threshold (Φ_c = 10.1 %). A contrasting effect of the fibers was seen when comparing the degradation kinetics of the biocomposites in freshwater and mature compost. In the first case, above Φ_c the fibers triggered hydrolysis and accelerated the degradation of the host PLA despite some nucleating action. Interestingly, the crystalline domains were also attacked after only 50 days of immersion at 45 °C. Swelling of the wet fibers and the weak fiber-matrix interface are also thought to play a role, likely creating water-rich pockets that are continuously fed by the external environment. Overall, in mature compost the degradation of the PLA was generally faster than in water due to the biotic environment and the higher temperature of the medium (ca. 55 °C) Regarding the effect of the fibers, they initially accelerated

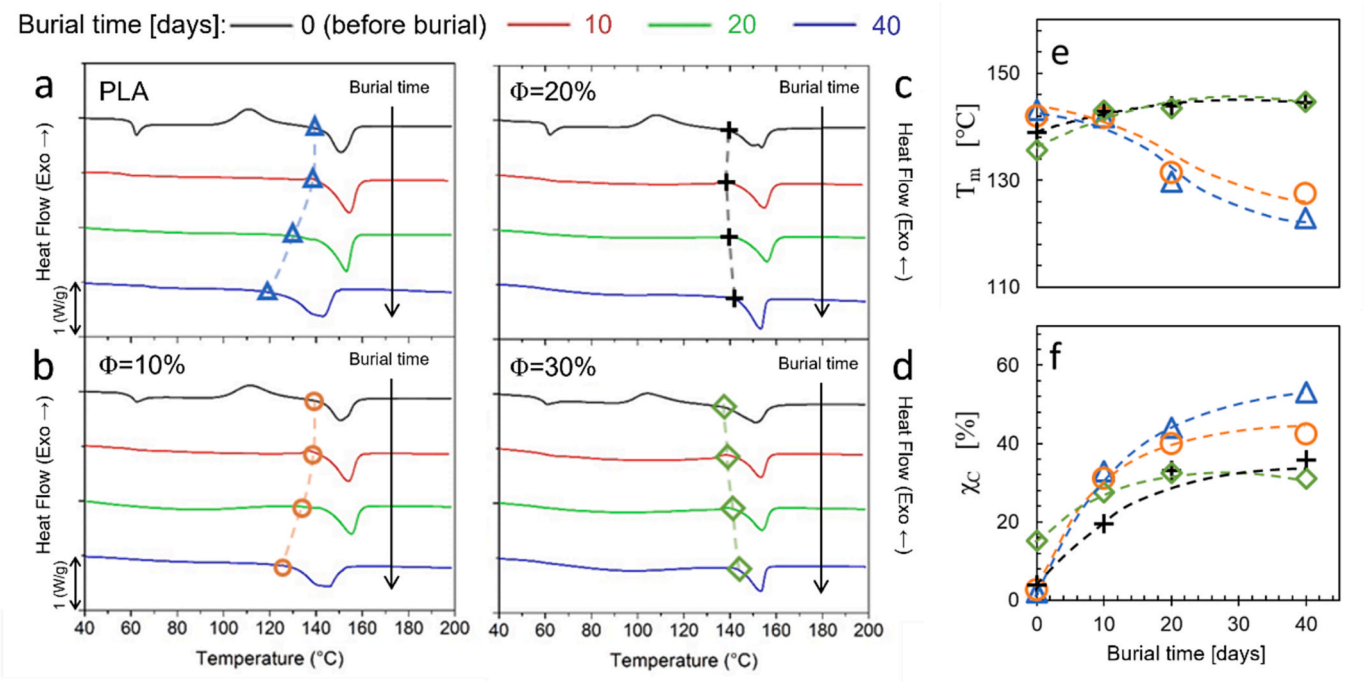

Fig. 9. DSC curves of PLA (a) and composites with Φ = 10 % (b), 20 % (c) and 30 % (d) of fibers as a function of burial time. The onset of melting temperature and the degree of crystallinity are also shown in (e) and (f), respectively: PLA (blue triangles) and composites with Φ = 10 % (orange circles), 20 % (black plus) and 30 % (green diamonds). Dashed lines in (e) and (f) are guides for the eye.

hydrolysis leading to a significant surface erosion of the biocomposites after only 10 days. However, over longer burial times the degradation kinetics of the pure PLA was faster, apparently due to the shielding effect of fiber-induced crystallinity. Finally, it is worth noting that, besides being beneficial on the biodegradation kinetics, which is the main end-of-life option for biocomposites, the selected fibers also ensure a slight enhancement of the flexural modulus of the biocomposites (Supplementary material, S3). Such a result potentially enables material saving, increasing the environmental sustainability of the studied systems also during the transport and use phase of their life cycle.

Finally, it is worth mentioning that the selected fibers not only have a positive influence on the biodegradation kinetics, which obviously has a positive effect on the end-of-life of the biocomposites, but also provide a slight improvement in the flexural modulus (Supplementary material, S3). Such a result enables material savings and increases the environmental sustainability of the studied systems also during the transportation and use phase of their life cycle.

CRediT authorship contribution statement

Libera Vitiello: Writing – original draft, Methodology, Investigation, Data curation. **Sabrina Carola Carroccio:** Writing – review & editing, Funding acquisition. **Veronica Ambrogi:** Writing – review & editing. **Edoardo Podda:** Investigation, Data curation. **Giovanni Filippone:** Writing – review & editing, Supervision, Funding acquisition, Formal analysis, Conceptualization. **Martina Salzano de Luna:** Writing – review & editing, Writing – original draft, Formal analysis.

Declaration of competing interest

The authors declare that they have no known competing financial interests or personal relationships that could have appeared to influence the work reported in this paper.

Data availability

Data will be made available on request.

Acknowledgments

We acknowledge financial support under the National Recovery and Resilience Plan (NRRP), Mission 4, Component 2, Investment 1.1, Call for tender No. 104 published on 02.02.2022 by the Italian Ministry of University and Research (MUR), funded by the European Union - NextGenerationEU- Project Title “Untapping the potential of GREEN COmposites by combining performance and environmental sustainability - GREENCO”, grant number 20223LWKTC, grant assignment decree No. 966 adopted on 30/06/2023 by MUR.

References

[1] L. Operato, L. Vitiello, A. Aprea, V. Ambrogi, M. Salzano de Luna, G. Filippone, Life cycle assessment of poly (lactic acid)–based green composites filled with pine needles or kenaf fibers, J. Clean. Prod. 387 (2023) 135901.
[2] T. Moshood, G. Nawanir, F. Mahmud, F. Mohamad, M. Ahmad, A. AbdulGhani, Sustainability of biodegradable plastics: new problem or solution to solve the global plastic pollution? Curr. Opin. Green Sustainable Chem. 5 (2022) 100273.
[3] T. Haider, C. Volker, J. Kramm, K. Landfester, F. Wurm, Plastics of the future? The impact of biodegradable polymers on the environment and on society, Angew. Chem. Int. Ed. 58 (1) (2019) 50–62.
[4] P. Russo, G. Simeoli, L. Vitiello, G. Filippone, Bio-polyamide 11 hybrid composites reinforced with basalt/flax interwoven fibers: a tough green composite for semi-structural applications, Fibers 7 (5) (2019) 41.
[5] M. Karamanlioglu, R. Preziosi, G. Robson, Abiotic and biotic environmental degradation of the bioplastic polymer poly(lactic acid): a review, Polym. Degrad. Stabil. 137 (2017) 122–130.
[6] P. Souza, A. Morales, M. Marin–Morales, L. Mei, PLA and montmorilonite nanocomposites: properties, biodegradation and potential toxicity, J. Polym. Environ. 21 (2013) 738–759.
[7] R. Auras, B. Harte, S. Selke, An overview of polylactides as packaging materials, Macromol. Biosci. 4 (9) (2004) 835–864.
[8] H. Henton, P. Gruber, J. Lunt, J. Randall, Natural fibers, biopolymers and biocomposites, in: A.K. Mohanty, M. Misra, L.T. Drzal (Eds.), Chapter 16, Polylactic Acid Technology, Taylor & Francis, Boca Raton, 2005.
[9] P. Stloukal, S. Pekarova, A. Kalendova, H. Mattausch, S. Laske, C. Holzer, L. Chitu, S. Bondner, G. Maier, M. Slouf, M. Koutny, Kinetics and mechanism of the

biodegradation of PLA/clay nanocomposites during thermophilic phase of composting process, Waste Manag. 42 (2015) 31–40.
[10] A. Bher, Y. Cho, R. Auras, Boosting degradation of biodegradable polymers, Macromol. Rapid Commun. 44 (5) (2023) 2200769.
[11] E. Castro-Aguirre, R. Auras, S. Selke, Impact of nanoclays on the biodegradation of poly (lactic acid) nanocomposites, Polymers 10 (2) (2018) 202.
[12] Z. Azwa, B. Yousif, A. Manalo, W. Karunasena, A review on the degradability of polymeric composites based on natural fibres, Mater. Des. 47 (2012) 424–442.
[13] M. Ja, M. Majid, M. Afendi, H. Marzuki, E. Hilmi, I. Fahmi, A.G. Gibson, Effects of water absorption on Napier grass fibre/polyester composites, Compos. Struct. 144 (2016) 138–146.
[14] M. Hubbe, N. Lavoine, L.A. Lucia, C. Dou, Formulating bioplastic composites for biodegradability, recycling, and performance: a review, Bioresources 16 (1) (2021) 2021–2083.
[15] C. Sun, H. Tan, Y. Zhang, Simulating the pyrolysis interactions among hemicellulose, cellulose and lignin in wood waste under real conditions to find the proper way to prepare bio-oil, Renew. Energy 205 (2023) 851–863.
[16] R. Scaffaro, A. Maio, E.F. Gulino, Hydrolytic degradation of PLA/Posidonia Oceanica green composites: a simple model based on starting morpho-chemical properties, Compos. Sci. Technol. 213 (2021) 108930.
[17] H.J. Kim, Y.H. Choi, J.H. Jeong, H. Kim, H.S. Yang, S.Y. Hwang Sy, J.M. Koo, Y. Eom, Rheological percolation of cellulose nanocrystals in biodegradable poly (butylene succinate) nanocomposites: a novel approach for tailoring the mechanical and hydrolytic properties, Macromol. Res. 29 (10) (2021) 720–726.
[18] R. Masirek, Z. Kulinski, D. Chionna, E. Piorkowska, M. Pracella, Composites of poly (L-lactide) with hemp fibers: morphology and thermal and mechanical properties, J. Appl. Polym. Sci. 105 (11) (2007) 255–268.
[19] W. Limsukon, R. Auras, T. Smith, Effects of the three–phase crystallization behavior on the hydrolysis of amorphous and semicrystalline poly (lactic acid) s, ACS Appl. Polym. Mater. 3 (11) (2021) 5920–5931.
[20] R. Auras, L. Lim, S. Selke, H. Tsuji, Poly (Lactic Acid): Synthesis, Structures, Properties, Processing, and Applications, vol. 10, John Wiley & Sons, Hoboken, New Jersey, 2011.
[21] G. Gorrasi, R. Pantani, Effect of PLA grades and morphologies on hydrolytic degradation at composting temperature: assessment of structural modification and kinetic parameters, Polym. Degrad. Stabil. 98 (2013) 1006–1014.
[22] N. Stevulova, J. Cigasova, A. Estokova, E. Terpakova, A. Geffert, F. Kacik, E. Singovszka, M. Holub, Properties characterization of chemically modified hemp hurds, Materials 7 (12) (2014) 8131–8150.
[23] L. Vitiello, M. Salzano de Luna, V. Ambrogi, G. Filippone, A simple rheological method for the experimental assessment of the fiber percolation threshold in short fiber biocomposites, Compos. Sci. Technol. (2023) 110345.
[24] E. Fukada, Piezoelectricity of biopolymers, Biorheology 32 (6) (1995) 593–609.
[25] L. Lim, R. Auras, M. Rubino, Processing technologies for poly (lactic acid), Prog. Polym. Sci. 33 (8) (2008) 820–852.
[26] W. Cai, L. Tremblay, L. An, Enhancing consumption responsibility to address global plastic pollution, Mar. Pollut. Bull. 138 (2022) 114089.
[27] V. Nagarajan, K. Zhang, M. Misra, A. Mohanty, Overcoming the fundamental challenges in improving the impact strength and crystallinity of PLA biocomposites: influence of nucleating agent and mold temperature, ACS Appl. Mater. Interfaces 7 (21) (2015) 11203–11214.
[28] M. Hakkarainen, Aliphatic polyesters: abiotic and biotic degradation and degradation products, Degradable aliphatic polyesters (2002) 113–138.
[29] E. Fischer, H. Sterzel, G. Wegner, Investigation of the structure of solution grown crystals of lactide copolymers by means of chemical reactions, Kolloid-Z. Z. Polym. 251 (11) (1973) 980–990.
[30] K. Fukushima, D. Tabuani, M. Dottori, I. Armentano, J. Kenny, G. Camino, Effect of temperature and nanoparticle type on hydrolytic degradation of poly (lactic acid) nanocomposites, Polym. Degrad. Stabil. 96 (2) (2011) 2120–2129.
[31] M. Elsawy, K. Kim, J. Park, A. Deep, Hydrolytic degradation of polylactic acid (PLA) and its composites, Renew. Sustain. Energy Rev. 79 (2017) 1346–1352.
[32] L. Husárová, S. Pekařová, P. Stloukal, P. Kucharzcyk, V. Verney, S. Commereuc, A. Ramone, M. Koytny, Identification of important abiotic and biotic factors in the biodegradation of poly (l–lactic acid), Int. J. Biol. Macromol. 71 (2014) 155–162.
[33] K. Fukushima, D. Tabuani, M. Dottori, I. Armentano, J. Kenny, G. Camino, Effect of temperature and nanoparticle type on hydrolytic degradation of poly (lactic acid) nanocomposites, Polym. Degrad. Stabil. 96 (2) (2011) 2120–2129.
[34] M. Sedničková, S. Pekařová, P. Kucharczyk, J. Bočkaj, I. Janigová, A. Kleinová, D. Jochec-Mošková, L. Omaníková, D. Perďochová, M. Koutný, V. Sedlařík, P. Alexy, I. Chodák, Changes of physical properties of PLA–based blends during early stage of biodegradation in compost, Int. J. Biol. Macromol. 113 (2018) 434–442.